

## Stability of Brain Intracellular Lactate and $^{31}\text{P}$ -Metabolite Levels at Reduced Intracellular pH During Prolonged Hypercapnia in Rats

‡Yoram Cohen, ‡Lee-Hong Chang, \*†¶Lawrence Litt, \*Francis Kim, \*¶John W. Severinghaus, §Philip R. Weinstein, ¶Richard L. Davis, §Isabelle Germano, and †‡Thomas L. James

Departments of \*Anesthesia, †Radiology, ‡Pharmaceutical Chemistry, §Neurosurgery, and ¶Pathology and ¶Cardiovascular Research Institute, University of California, San Francisco, California, U.S.A.

**Summary:** The tolerance of low intracellular pH ( $\text{pH}_i$ ) was examined in vivo in rats by imposing severe, prolonged respiratory acidosis. Rats were intubated and ventilated for 10 min with 20%  $\text{CO}_2$ , for 75 min with 50%  $\text{CO}_2$ , and for 10 min with 20%  $\text{CO}_2$ . The maximum  $\text{P}_a\text{CO}_2$  was 320 mm Hg. Cerebral intracellular lactate,  $\text{pH}_i$ , and high-energy phosphate metabolites were monitored in vivo with  $^{31}\text{P}$  and  $^1\text{H}$  nuclear magnetic resonance (NMR) spectroscopy, using a 4.7-T horizontal instrument. Within 6 min after the administration of 50%  $\text{CO}_2$ ,  $\text{pH}_i$  fell by  $0.57 \pm 0.03$  unit, phosphocreatine decreased by ~20%, and  $\text{P}_i$  increased by ~100%. These values were stable throughout the remainder of the hypercapnic period. Cerebral intracellular lactate, visible with  $^1\text{H}$  NMR spectroscopy in the hyperoxic state, decreased during hypercapnia, suggesting either a favorable change in oxygen availability (decreased lactate production) or an increase in lactate clearance or both. All hypercapnic animals awakened and behaved normally after  $\text{CO}_2$  was discontin-

ued. Histological examination of cortical and hippocampal areas, prepared using a hematoxylin and eosin stain, showed no areas of necrosis and no glial infiltrates. However, isolated, scattered, dark-staining, shrunken neurons were detected both in control animals (no exposure to hypercapnia) and in animals that had been hypercapnic. This subtle histological change could represent an artifact resulting from imperfect perfusion-fixation, or it could represent subtle neurologic injury during the hypercapnia protocol. In summary, extreme hypercapnia and low  $\text{pH}_i$  (~6.5) are well tolerated in rats for periods up to 75 min if adequate oxygenation is maintained. The prolonged stability of metabolite concentrations during hypercapnia makes its use convenient for in vivo animal studies of the relevance of  $\text{pH}_i$  to brain injury. **Key Words:** Carbon dioxide—Energy metabolism—Hypercapnia—Intracellular pH—Lactate—Nuclear magnetic resonance spectroscopy.

Although ischemic injury to neural tissue invariably occurs at low intracellular pH ( $\text{pH}_i$ ), numerous in vitro studies suggest that low  $\text{pH}_i$  is a cause, and not simply a result, of deleterious biochemical processes. For example, in vitro studies have shown that the following processes can be disturbed by intracellular acidosis: (a) transmembrane ion homeostasis (Siesjö, 1985); (b) cell volume regulation (Siesjö, 1985); (c) mitochondrial and cytosolic metabolism (Hillered et al., 1984); (d) intracellular cal-

cium management; and (e) free radical scavenging (Rehncrona et al., 1989), lipid peroxidation (Siesjö et al., 1985), and iron homeostasis (Barber and Bernheim, 1976). Nevertheless, rapid clinical recovery from severe, acute respiratory acidosis is a recognized phenomenon that demonstrates the ability of animals and humans to tolerate low  $\text{pH}_i$  in vivo. During a previous  $^{31}\text{P}$  nuclear magnetic resonance (NMR) spectroscopy study in rats, brain  $\text{pH}_i$  and ATP changes were measured in vivo during brief periods of severe hypercapnia (Litt et al., 1985). All rats recovered metabolically and neurologically from severe hypercapnia caused a 0.65-unit decrease in  $\text{pH}_i$ . In the present study we have employed  $^{31}\text{P}$  and  $^1\text{H}$  NMR spectroscopy to investigate if prolonged hypercapnic increases in intracellular hydrogen ion concentrations are toler-

Received May 25, 1989; revised September 16, 1989; accepted September 21, 1989.

Address correspondence and reprint requests to Dr. L. Litt at Department of Anesthesia, UCSF Box 0648, San Francisco, CA 94143, U.S.A.

**Abbreviations used:** CK, creatine kinase; NMR, nuclear magnetic resonance; PCr, phosphocreatine; PME, phosphomonoesters.

ated without subsequent cerebral metabolic failure and tissue injury. We hypothesize that the maintenance of adequate tissue oxygenation permits prolonged tolerance of low  $pH_i$  values that are usually associated with cerebral metabolic failure.

### BACKGROUND

Animal and human studies demonstrated whole-body metabolic and physiologic tolerance of hypercapnia (Hopkins et al., 1954; Clowes et al., 1955; Frumin et al., 1959) long before technological advances in NMR spectroscopy made it possible to noninvasively measure brain  $pH_i$  in vivo. During the last few years, however, in vivo  $^{31}\text{P}$  NMR spectroscopy, which permits repeated, noninvasive metabolite determinations from the same tissue over long periods of time, has been used to reexplore brain acid-base phenomena (Behar et al., 1987; Nioka et al., 1987), the study of which previously required the use of additional animals and invasive techniques. Two principal differences exist between in vivo NMR spectroscopy measurements and invasive determinations from excised tissues. Qualitatively, in vivo NMR spectroscopy detects only those unbound (or loosely bound) compounds that are in solution, free to participate in biochemical reactions. Quantitatively, in vivo NMR spectroscopy fails to directly detect compounds whose concentration is less than  $\sim 0.5$  mM, and therefore it is usually  $\sim 1,000$ -fold less sensitive than other biochemical assays. The  $^{31}\text{P}$  NMR technique for  $pH_i$  determinations is based on inferring nanomolar concentrations from an indirect determination of the relative concentrations of monobasic and dibasic inorganic phosphate ( $P_i$ ). It has been described previously (Moon and Richards, 1973; Petroff et al., 1985), and it has also been used recently to measure rat brain buffering capacity in vivo (Adler et al., 1988).

A previous  $^{31}\text{P}$  NMR investigation by us demonstrated that mechanically ventilated rats will tolerate acute, 15-min periods of supercarbia ( $P_a\text{CO}_2 > 500$  mm Hg) when their blood oxygen saturation is  $>80\%$  (Litt et al., 1985). On the one hand, supercarbia also produces general anesthesia equivalent to that caused by  $\sim 2\%$  halothane, and cerebral metabolic demand is reduced (Eisele et al., 1967). On the other, supercarbia also causes brain  $pH_i$  to decrease by 0.65 pH unit, an amount comparable to the decrease that occurs in rats after an injurious 15-min occlusion of both carotid and both vertebral arteries (Mabe et al., 1983). Previous invasive studies of brain intracellular metabolite changes during hypercapnia indicate that concentrations of glyco-

lytic and tricarboxylic acid cycle intermediates continue to change for 45 min after the start of  $\text{CO}_2$  administration (Folbergrová and Siesjö, 1973). We therefore decided to use NMR spectroscopy to explore in vivo metabolic changes during extended periods of hypercapnia ( $P_a\text{CO}_2 \approx 320$  mm Hg). Our goals were to determine (a) if NMR-observable brain  $^{31}\text{P}$ - and  $^1\text{H}$ -metabolites are stable during severe hypercapnic periods that are long enough to allow all biochemical changes to reach a steady state and (b) if recovery from prolonged hypercapnia is characterized by abnormal neurologic outcome or by delayed histological injury.

### METHODS

Experiments were performed with the approval of the UCSF Committee on Animal Research. Similar  $\text{CO}_2$  administration protocols were followed in invasive nonsurvival studies and in noninvasive survival studies. In all cases Sprague-Dawley rats weighing 300–350 g had anesthesia induced in a chamber containing isoflurane (3%) and  $\text{O}_2$  (97%). When spontaneous respirations became shallow, the animals were removed from the chamber and orotracheal intubation was performed quickly and atraumatically. Mechanical ventilation with isoflurane/ $\text{O}_2$  (1.5:98.5%) was instituted, and 0.25 mg of pancuronium was given by intraperitoneal injection. A rectal thermometer and a heating pad were used to monitor and control body temperature.

No surgery was performed in one group of seven rats that underwent in vivo  $^{31}\text{P}$  NMR spectroscopic studies. Parallel studies were conducted in two rats having femoral intravascular catheters to verify that expected changes in arterial blood gas measurements occurred in association with 50%  $\text{CO}_2$  administration. Blood pressure and heart rate were also measured in the parallel studies to determine whether cardiovascular stability prevailed with time during hypercapnia. Animals in the NMR studies were placed on a Plexiglas frame, and an elliptical (14 × 11 mm), two-turn, double-tuned ( $^1\text{H}$ ,  $^{31}\text{P}$ ) surface coil was placed on the head, above the brain. The animal/Plexiglas assembly was placed in the horizontal bore of our 4.7-T NMR instrument ( $^{31}\text{P}$  resonance frequency = 81.005 MHz), a Quest 4300 made by the Nalorac Corp. Magnetic field homogeneity was optimized by adjusting room temperature shim currents until the line width of the  $^1\text{H}$  resonance of water (200.1 MHz) was  $\leq 30$  Hz.

Four different  $^{31}\text{P}$  "control spectra" were obtained at the beginning of each experiment. The first was collected with a 1.8-s recycle time. It averaged 180 acquisitions and had a total collection time of  $\approx 6$  min/spectrum. The second, a "fully relaxed"  $^{31}\text{P}$  spectrum, was collected with a 15-s recycle time. It averaged 120 acquisitions and had a collection time of  $\sim 30$  min. In each experiment the "fully relaxed" spectrum was analyzed on-line to verify that the measured phosphocreatine (PCr)/ATP ratio was that for brain ( $1.8 \pm 0.1$ ). The third and fourth control spectra, and all subsequent  $^{31}\text{P}$  spectra, were taken using the same NMR parameters as the first control spectrum.

Other  $^{31}\text{P}$  NMR spectroscopic details include the fact that the spectral width was  $\pm 3,125$  Hz, and 4K complex

data points were sampled. The digital resolution was 1.5 Hz/point. The broad  $^{31}\text{P}$  background from bone and phospholipids was reduced with selective presaturation. Intracellular pH was determined from the chemical shift difference between  $\text{P}_i$  and PCr resonance peaks (Petroff et al., 1985). Relative intracellular metabolite concentrations were obtained by the integration of curves fitted to individual metabolite peaks. During the analysis procedure, the remaining broad component was fitted as a separate peak.

$^{31}\text{P}$  NMR experiments began with the taking of control spectra during normocapnic isoflurane anesthesia. Thereafter the inspired isoflurane concentration was reduced to 0.5% and the inspired  $\text{CO}_2$  concentration was raised to 20%. After a waiting period of 2 min, another  $^{31}\text{P}$  NMR spectrum was recorded. After a second waiting period of 2 min, the inspired  $\text{CO}_2$  concentration was then raised to 50% and isoflurane was turned off. Twelve more spectra were acquired. Each NMR study was completed in two additional stages. First, the inspired  $\text{CO}_2$  concentration was decreased to 20% and the isoflurane concentration was restored to 0.5%. Second, after 10 min the inspired  $\text{CO}_2$  was discontinued and 1.5% isoflurane was restored. Seven recovery  $^{31}\text{P}$  spectra (no  $\text{CO}_2$  administration, 1.5% isoflurane administration, 6 min/spectrum) were obtained during a 45-min period.

After the NMR studies, the animals were removed from the magnet, placed supine, and given ventilatory support with 100% oxygen until spontaneous respirations were noted. When adequate breathing was apparent, the ventilator was disconnected but the endotracheal tube was left in place. The animals were permitted to awaken and extubate themselves. The same  $\text{CO}_2$  protocol was repeated in separate animals during  $^1\text{H}$  NMR studies.

$^1\text{H}$  NMR spectroscopy experiments were also performed in six animals, using a single-tuned  $12 \times 15\text{-mm}$  elliptical surface coil. The spectral width was  $\pm 3,125$  Hz, and 4K complex data points were sampled. The acquisition time was 655.4 ms, and the interpulse delay was 1.0 s. Suppression of the large  $^1\text{H}$  signal from water was accomplished with a presaturation pulse 0.1 s in duration. The in vivo  $90^\circ$  pulse was  $20 \pm 2 \mu\text{s}$  for each of the experiments. The  $^1\text{H}$  NMR signal at 1.32 ppm from the methyl protons in lactate was selectively inverted in a  $J$ -coupling spin echo experiment to distinguish it from noninverted residual lipid signals (Chang et al., 1987). Four of the six animals had no surgery and were allowed to recover consciousness and survive 1 week. In two animals the scalp was excised and the temporal muscles were retracted laterally from the cranium. For the rats that had no surgery, a long echo delay [ $\tau = 3(1/2J) = 204$  ms] was needed to eliminate lipid resonances. The recycle time in these experiments was 2.16 s, and 120 scans were averaged for each spectrum, resulting in a collection time of  $\approx 4.33$  min/spectrum. For the rats that had surgery, an effective reduction of the size of lipid resonances could be achieved with a shorter  $\tau$  value ( $1/2J = 68$  ms) and a correspondingly shorter collection time,  $\sim 3.79$  min/spectrum. In these rats  $^1\text{H}$  NMR spectra were alternately acquired using both echo delays ( $\tau = 68$  and 204 ms). The time course of lactate concentrations throughout the experiment was compared in the two sets of spectra.

Additional studies were conducted to verify that the inverted  $^1\text{H}$  signal at 1.32 ppm was from lactate in brain. First, one-dimensional spectroscopic imaging experi-

ments were performed with the same surface coil using a pulse sequence recently described by our group (Cohen et al., 1989). The spectroscopic imaging sequence permitted concomitant acquisition of signals from a series of slices, 1 mm thick, through the head. Second, responses to brief periods of hypoxia ( $\approx 3$  min of  $\text{P}_{\text{aO}_2}$  of  $\approx 20$  mm Hg) were studied in two sets of animals; those with and without surgery. Third, spectra were also obtained with the detection coil located over retracted muscle.

Histological studies were conducted in four animals that recovered from hypercapnia. Two rats were observed for 1 week, anesthetized with ketamine (100 mg/kg i.p.), and killed by intraaortic perfusion fixation with formalin (10%). Two others were killed after 4 weeks.

Pathology specimens were obtained according to the following procedure. Ketamine anesthesia was achieved. Thereafter a midline thoracotomy was performed, and a right ventricular drain was placed. The descending aorta was then cross-clamped at the level of the diaphragm. The left ventricle was opened and a ball-tipped metal needle, normally used for gavage feedings, was inserted firmly into the ascending aorta. Heparinized saline was flushed into the aorta until the right ventricular drain returned clear fluid. Formalin (10%,  $\approx 120$  ml) was then injected slowly under constant pressure into the aorta and noted to return from the right ventricular drain. The animals were then decapitated, and the perfused heads, submerged in formalin, were allowed to fix in situ for 2 days. Both cerebral hemispheres and the cerebellum were then removed and fixed in formalin for 3 more days. Thereafter the brains were sectioned coronally into 3-mm-thick slices, processed in graded ethanol and xylol, and embedded in paraffin. Serial sections 6  $\mu\text{m}$  thick were made using a Leitz 1512 rotary microtome. Representative slices showing cortical, hippocampal, and deep nuclear regions were then selected for histopathological staining with hematoxylin and eosin and acid fuchsin. Control slides for histopathology studies were obtained from brain slices in (a) two animals that underwent perfusion-fixation without any exposure to hypercapnia and (b) one animal that, as part of another experimental protocol, had survived 1 week after an ischemic insult in the distribution of a middle cerebral artery. After tissue preparation and histological staining, slides were examined for the following morphological changes associated with neuronal damage: microvacuolization, shrunken dark nuclei, incrustations, and glial infiltrates and changes.

## RESULTS

Representative  $^{31}\text{P}$  NMR brain spectra are shown in Fig. 1. Figure 2A shows the  $\text{pH}_i$  behavior throughout the  $^{31}\text{P}$  experiments for seven animals. The  $\text{pH}_i$  decrease was  $0.57 \pm 0.03$  pH unit 6 min after the administration of 50%  $\text{CO}_2$ . Arterial pH in the parallel experiments fell to the same value, as one would expect from  $\text{CO}_2$  equilibration into all tissue compartments. This equilibration is exhibited in Fig. 2B, which compares average intracellular and arterial pH changes. Figure 3, which shows  $^{31}\text{P}$ -metabolite changes relative to their control values before  $\text{CO}_2$  administration, displays the con-

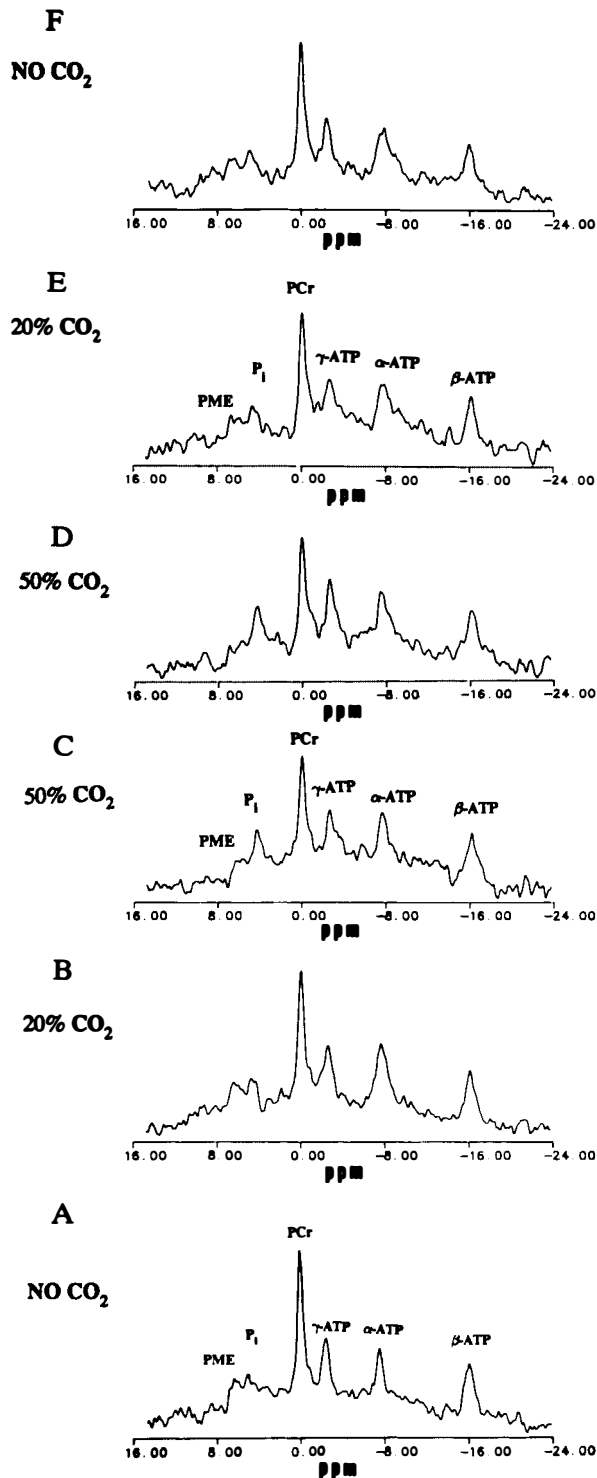


**FIG. 1.** Representative  $^{31}\text{P}$  nuclear magnetic resonance spectra in one animal before, during, and after hypercapnia. A one-pulse technique was used, with selective presaturation of the broad lipid background. All spectra represent averages of 180 excitations, taking a total collection time of 6 min. **A:** The first control spectrum; **B:** during the initial administration of 20%  $\text{CO}_2$ ; **C:** during the first 6 min of 50%  $\text{CO}_2$  administration, corresponding to  $\text{P}_a\text{CO}_2 = 320$  mm Hg; **D:** during the last 6 min of 50%  $\text{CO}_2$  administration; **E:** during 20%  $\text{CO}_2$  administration following severe hypercapnia; **F:** 45 min after  $\text{CO}_2$  administration was discontinued. PME, phosphomonoesters; PCr, phosphocreatine.

stancy of intracellular ATP throughout the experiment. This figure also shows that the average decrease in PCr was  $\approx 20\%$ , while the average increase in  $\text{P}_i$  was  $\approx 100\%$ . Figure 4 shows the behavior of  $\text{PCr}/\text{P}_i$  for each of the animal studies. Saturation corrections for  $T_1$  relaxation have not been applied to any of the figures or metabolite ratios.

Figures 2–4 clearly demonstrate that new  $^{31}\text{P}$ -metabolite values were achieved within 10 min after the start of hypercapnia and that  $^{31}\text{P}$ -metabolite concentrations and intracellular pH were stable throughout the next hour of the NMR experiments. After restoration of 100%  $\text{O}_2$ , metabolite concentrations returned to their control values.

Cardiovascular parameters were also stable in the parallel experiments. Gross neurologic recovery after 75 min of hypercapnia appeared to be complete 4 h after the episode and maintained for weeks after the experiment.

In Fig. 2 we note that the recovery rate for  $\text{pH}_i$  varies slightly from animal to animal. The one rat that did not show a total  $\text{pH}_i$  recovery after 45 min did, however, exhibit normal behavior 4 h after the hypercapnia episode.

The results of a typical  $^1\text{H}$ -lactate study are shown in Fig. 5. For the rats that had no surgery ( $\tau = 204$  ms), intracellular lactate was visible in the hyperoxic control state (where lactate concentrations are typically small, e.g.,  $\approx 1$  mM). Observed lactate signals decreased to nonobservable values during well-oxygenated hypercapnia. During recovery from hypercapnia, intracellular lactate increased above the control value, reaching a maximum value 15–20 min into the recovery period and thereafter gradually decreasing to control values, which were reached  $\approx 45$  min after recovery began. The lactate/*N*-acetylaspartate ratios are summarized in Table 1.

Data from the special studies verified that the signal at 1.32 ppm, attributable to lactate, came from the brain. First, in two animals that had surgery and in two that did not, a 6-min period of hypoxia was induced after shimming was completed and control  $^1\text{H}$  NMR spectra were obtained.  $\text{P}_a\text{O}_2$  was reduced from  $\approx 500$  to  $\approx 20$  mm Hg. The magnitude of the inverted signal at 1.32 ppm was seen to increase and then return to its original value after  $\text{P}_a\text{O}_2$  was restored to control. Second, for two animals that had surgery, two series of spin echo  $^1\text{H}$  spectra were obtained in the same animal for the entire hypercapnia protocol. The spectra were interleaved, and pulsing parameters were the same except for the spin echo delay. Two values of  $\tau$  were used: 68 and 204 ms. The same behavior of the lactate peak was seen in both sets of spectra. The lactate resonance

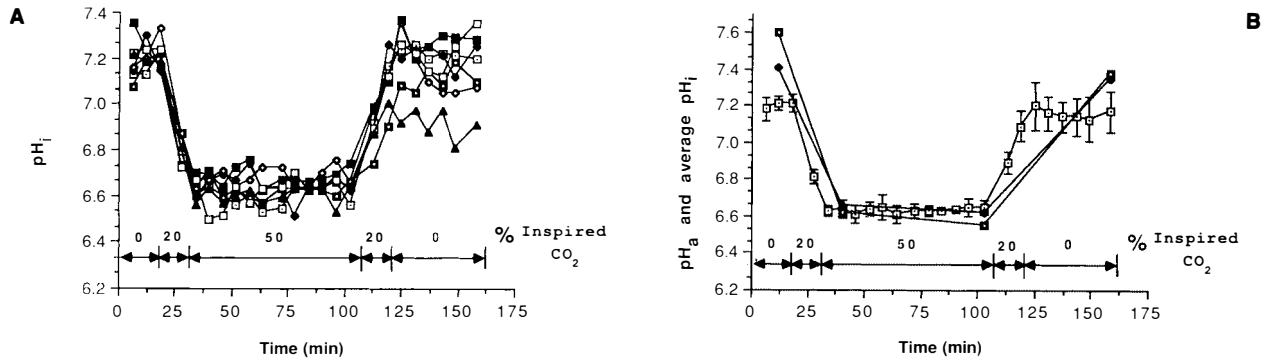


**FIG. 2.** Cerebral intracellular pH ( $pH_i$ ) before, during, and extreme hypercapnia. **A:** The data for each of the seven animals; **B:** the average  $pH_i$  for seven animals ( $\square$ ) in the nuclear magnetic resonance studies and arterial blood gas values ( $\square$ ,  $\blacklozenge$ ) for two animals studied in parallel experiments. Errors are SDs.

behaved the same as in animals that had no surgery: (a) It was small during the hyperoxic control period; (b) it became smaller and disappeared during hypercapnia; and (c) it reappeared with a larger magnitude after hypercapnia was discontinued. Third, the more time-consuming one-dimensional spectroscopic imaging experiment was performed during hypercapnia in a rat that had no surgery, and the  $^1H$  spectrum from a 1-mm-thick region of the brain, centered at a 5-mm depth, exhibited the same lactate behavior during the  $CO_2$  protocol as was seen in the series where surgery was performed and different  $\tau$  values were used. Fourth, data were taken during hypercapnia in an animal that underwent surgery but had the coil placed over the temporalis muscles on one side of the head, instead of being centered on top of the head, over the brain. The muscle lactate signal was negligible. These four studies indicate that the lactate signal measured during the hypercapnia study originated in the brain.

Histologically, the hematoxylin and eosin preparations of the cerebrum of the two control animals

(no hypercapnia exposure) contained some areas having isolated, localized, shrunken, “dark-staining” neurons. No high-power field of the cortex having more than one dark neuron could be found. Occasional dark neurons could also be observed in the hippocampus, but never more than two per high-power field. Dark neurons were found with the same frequency in three of the four brains of animals that survived 2–4 weeks after hypercapnia. In these three animals, the number of dark neurons was the same as in the control group. One of the four animals, however, had noticeably more dark neurons, and one area of the hippocampus contained a high-power field with five, as shown in Fig. 6. The presence of “dark” neurons was rare, asymmetric bilaterally, and difficult to quantitate. They could represent either subtle injury or artifact: the well-known “dark” cell change that occurs during imperfect perfusion-fixation and handling (Cammeyer, 1961; Brierley, 1976; Brown, 1977).

No evidence of incrustations, microvacuolization, or glial infiltrates was ever found in any of the animals, including the control group. Acid fuchsin slides in the posthypercapnia group were also not

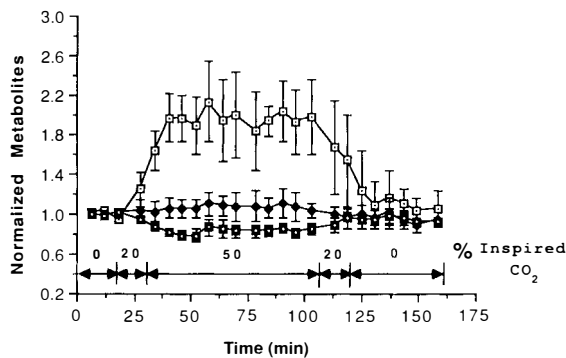


**FIG. 3.**  $^{31}P$ -Metabolite levels before, during, and after extreme hypercapnia. Each metabolite, measured as a percentage of its value in the control spectrum, was obtained from an average of six animals. Errors are SDs. ( $\blacklozenge$ ), ATP; ( $\square$ ),  $P_i$ ; ( $\square$ ), phosphocreatine.

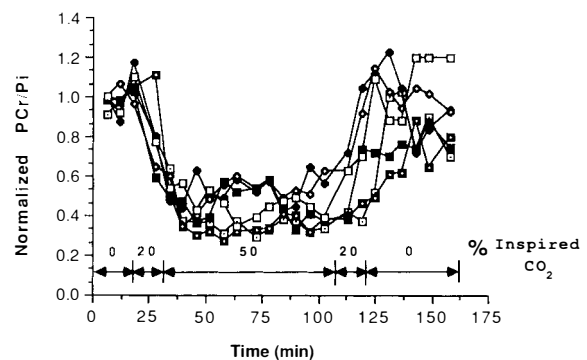


**FIG. 4.** The phosphocreatine (PCr)/ $P_i$  ratio measured relative to the PCr/ $P_i$  ratio during the control period. The data are shown for each animal.

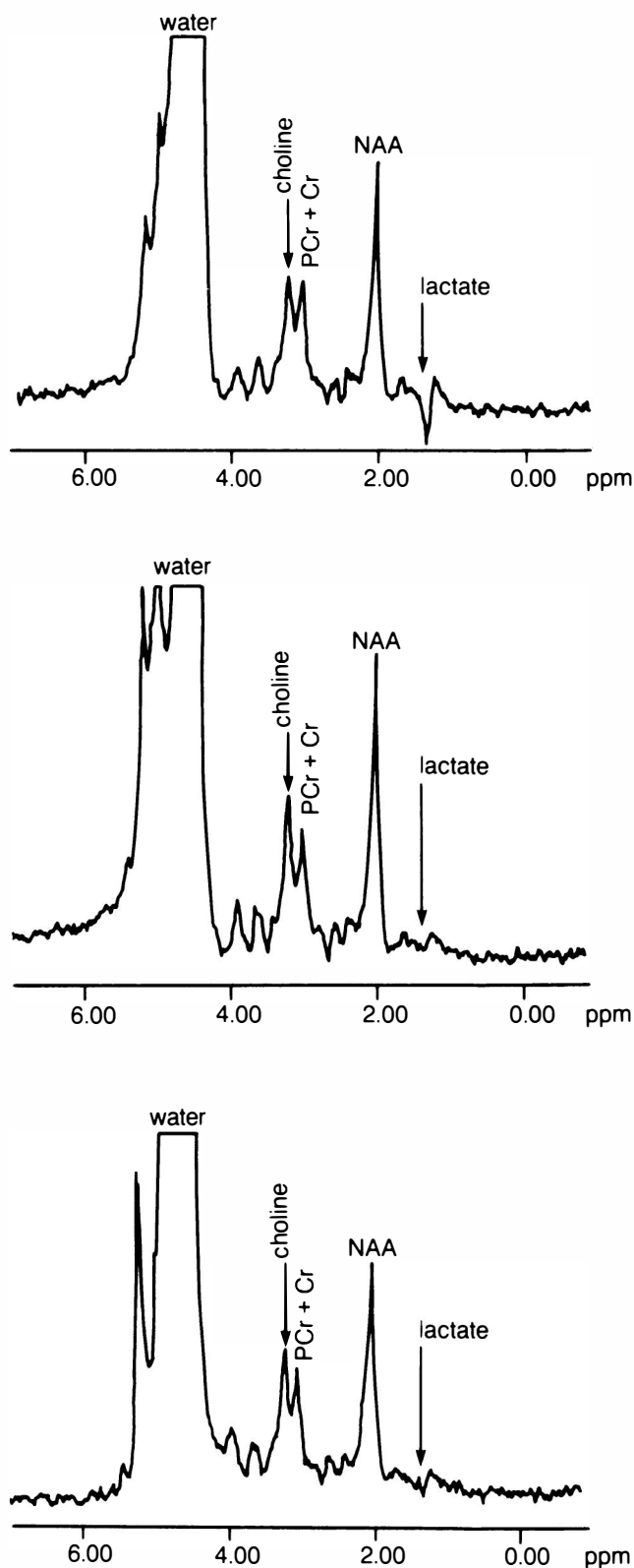


**FIG. 5.** Representative  $^1\text{H}$  nuclear magnetic resonance spectra from one animal before (**bottom**), during (**middle**), and 20 min after (**top**) hypercapnia. A water-suppressed spin echo sequence ( $\tau = 204$  ms) was used as described in the text. PCr, phosphocreatine; Cr, creatine; NAA, *N*-acetylaspartate.

**TABLE 1.** Lactate/*N*-acetylaspartate (NAA) nuclear magnetic resonance ratios before, during, and after hypercapnia

Time of spectral acquisition	Lactate/NAA
Control period	$0.071 \pm 0.005$
First 6 min of 50% $\text{CO}_2$	0.000 (lactate undetectable)
Last 6 min of 50% $\text{CO}_2$	0.000 (lactate undetectable)
14–20 min after hypercapnia	$0.155 \pm 0.013$
45 min after hypercapnia	$0.074 \pm 0.008$

Values are the averages of six animals.  $\tau = 204$  ms in the spin echo experiment. Errors are standard deviations of the mean.

significantly different from those obtained in control rats that were not exposed to  $\text{CO}_2$ .

## DISCUSSION

Extreme hypercapnia and low  $\text{pH}_i$  ( $\approx 6.6$ ) are tolerated in rats for periods of up to 75 min, and it appears that high-energy phosphate concentrations quickly attain new steady-state values. No gross neurobehavioral changes were apparent, nor were there substantial histological indications of injury. It is possible, but not certain, that the increase in dark neuron changes seen in one animal was indicative of  $\text{CO}_2$ -induced injury. Nevertheless, while the problems of dark neuron artifacts make it difficult to distinguish between inadequate perfusion-fixation and subtle injury, it is clear that any deficit resulting from the period of hypercapnia is minimal compared to that occurring during ischemia-induced decreases in  $\text{pH}_i$ .

We note that perfusion-fixation was always good in our preparations, because cerebral vessels were nearly always devoid of red blood cells. The perfection of our perfusion-fixation techniques, i.e., the adoption of a protocol that yields no ambiguities

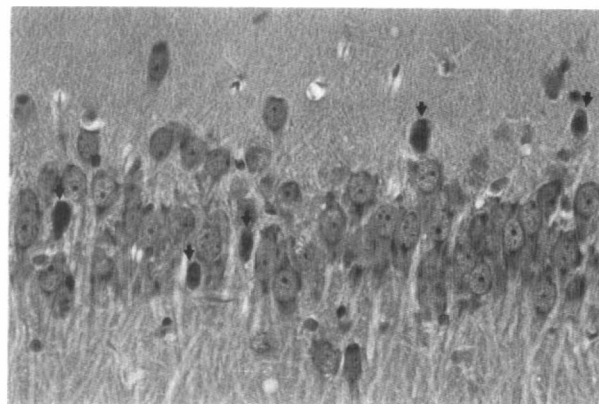


**FIG. 6.** Photograph of a high-power field showing dark-staining, shrunken neurons, indicated by arrows, in the granular layer of the hippocampus. Dark cells are compatible with either perfusion artifact or subtle injury as described in the text.

in the light microscopy studies, would also encourage us to conduct electron microscopy studies of ultrastructural responses, a more sensitive test for minimal injury (Bakay and Lee, 1968; Matakas et al., 1978).

The creatine kinase (CK) reaction,  $\text{PCr} + \text{ADP} + \text{H}^+ \leftrightarrow \text{Cr} + \text{ATP}$ , is at equilibrium during stable periods of hypercapnia. Thus, low  $\text{pH}_i$ , or increased  $\text{H}^+$ , drives the reaction to the right and results in decreased PCr. Hypercapnia, like ischemia, causes PCr to decrease and  $\text{P}_i$  to increase. In contrast to ischemia, however, hypercapnia with adequate oxygenation preserves ATP levels and causes changes in amino acid intermediate metabolites that are opposite to those occurring during cerebral ischemia. The shift of glycolytic and tricarboxylic acid cycle intermediates toward an "energy-rich" profile makes one expect that intracellular lactate should decrease during hypercapnia with adequate oxygenation.

Contemplation of the CK reaction leads to the noteworthy observation that hypercapnia-induced cerebral intracellular responses for  $\text{P}_i$ , PCr, and ATP are similar to exercise-induced changes in skeletal muscle (Taylor et al., 1983). Although different intracellular mechanisms predominate in the two tissue types, both situations have the CK reaction being driven to the right under circumstances where ATP can be maintained. During hypercapnia the CK reaction is pushed to the right by increased  $\text{H}^+$ ; during muscle work it is pushed to the right by increased  $\text{H}^+$  and increased ADP. Furthermore, as in the case of exercising muscle, the  $\text{pH}_i$  recovery seems to precede the recovery of the PCr/ $\text{P}_i$  ratio (cf. Figs. 2A and 4).

It is possible, as suggested *in vitro*, that hypoxic/ischemic increases in cerebral intracellular lactate cause a decrease in  $\text{pH}_i$ , and that this in turn causes deleterious metabolic modulations. Such modulations, however, are not apparent during prolonged hypercapnic states of reduced  $\text{pH}_i$ . To the contrary, there is a decrease in intracellular lactate during extreme hypercapnia that is consistent with luxury oxygenation of the brain. After hypercapnia, the transient increase in intracellular lactate above control that accompanies the return to normocapnia might have resulted from reduced CBF (i.e., from decreased oxygen availability) due to persisting bicarbonate generated during severe hypercapnia. In a study in dogs (Safar et al., 1973), it was shown that rapid normalization of  $\text{P}_a\text{CO}_2$  after hypercapnia increases extracellular pH, decreases cerebral blood flow, and causes increased lactate formation. One can only speculate in our experiment, however, because CBF and extracellular pH and  $\text{PCO}_2$

were not measured. Because intracellular pH is better buffered than extracellular pH, this issue is not resolved by the failure of  $\text{pH}_i$  to overshoot during the recovery period.

One can speculate that intracellular metabolic disturbances during cerebral acidosis are also related to disruptions of transmembrane  $\text{pH}_i$  gradients, and not only to decreases in absolute values of  $\text{pH}_i$ . For example, the important process of oxidative phosphorylation, explained by Mitchell's chemiosmotic hypothesis, requires a transmembrane proton gradient to return  $\text{H}^+$  through the membrane-bound enzyme  $\text{F}_0\text{F}_1\text{-ATPase}$  (Westhoff and van Dam, 1987). The response of intracellular pH gradients might be different during hypercapnia and hypoxia/ischemia. In the former condition  $\text{CO}_2$  diffuses across membranes before combining with  $\text{H}_2\text{O}$  to generate  $\text{H}^+$  and carbonate. In the latter situation different cytosolic and mitochondrial processes generate  $\text{H}^+$  ions, and  $\text{H}^+$  accumulation in the mitochondrion is augmented by decreased operation of an oxygen-deprived electron transport chain, and finally by decreased membrane integrity. *In vivo* NMR spectroscopy studies such as ours are not capable of assessing the importance of  $\text{pH}_i$  gradients. Perhaps quantitative examinations of their role will ultimately be permitted by new fluorescence microscopy techniques, which allow the mapping of  $\text{pH}_i$  distributions in single cells (Bright et al., 1987).

Because we associate the inverted  $^1\text{H}$  resonance at 1.32 ppm with lactate, we conclude that during hyperoxia, small concentrations of intracellular lactate ( $\sim 1 \text{ mM}$ ) are detectable *in vivo* with  $^1\text{H}$  NMR spectroscopy. The assignment of lactate to the inverted peak at 1.32 ppm requires justification at low lactate concentrations, because other compounds have similar chemical shift locations (ppm) and coupling constants (Hz). The methyl doublets of lactate (1.32 ppm, 7.3 Hz) resonate in proximity to those of alanine (1.46 ppm, 7.2 Hz),  $\beta$ -hydroxybutyrate (1.19 ppm, 9.1 Hz), and threonine (1.33 ppm, 6.1 Hz) (L. Bolinger et al., personal communication). However, the sharpness of our lactate resonance peaks ( $\nu_{\text{FWHM}} \leq 0.10 \text{ ppm}$ ) permits us to exclude contamination from alanine and  $\beta$ -hydroxybutyrate. Although the chemical shift of the methyl group of threonine is indistinguishable from that of the methyl group of lactate, the difference in the lactate and threonine coupling constants and our use of a long echo delay ( $\tau = 3/2J = 204 \text{ ms}$ ) result in an amplitude-reducing phase modulation of the methyl group of threonine, which has  $3/2J = 246 \text{ ms}$ . Thus, threonine is somewhat suppressed with our pulse sequence, although not totally. In princi-

ple, lactate could be distinguished in vivo at low concentrations by performing selective proton decoupling of either the  $\alpha$ -CH lactate resonance at 4.11 ppm or the  $\beta$ -CH threonine resonance at 4.25 ppm. In any case, the hypercapnia-induced decrease of the  $^1\text{H}$  resonance at 1.32 ppm rules out the possibility that lactate is increasing and thereby refutes the assertion that low  $\text{pH}_i$  per se impairs brain metabolism. Prolonged hypercapnia (90 min) is tolerable and neurologic function is recoverable, despite  $\text{pH}_i$  values of 6.6, considered low because they occur during stroke. The lowest tolerable  $\text{pH}_i$ , not known, seems determinable using the methods described in the present work. Further studies of the effects of low  $\text{pH}_i$  seem appropriate with this animal model.

**Acknowledgment:** Dr. Cohen acknowledges partial support by a Fulbright Scholarship, administered by the U.S.-Israel Educational Foundation. Other financial support is gratefully acknowledged from the National Institutes of Health (grants GM34767, RR03841, and CA44651).

## REFERENCES

- Adler S, Simplaceanu V, Ho C (1988) Determination of rat brain buffering in vivo by  $^{31}\text{P}$ -NMR. *J Appl Physiol* 64:1829-1836
- Bakay L, Lee JC (1968) The effect of acute hypoxia and hypercapnia on the ultrastructure of the central nervous system. *Brain* 91:697-706
- Barber AA, Bernheim F (1976) Lipid peroxidation: its measurement, occurrence, and significance in animal tissues. *Adv Gerontol Res* 2:355-403
- Behar KL, Rothman DL, Fitzpatrick SM, Hetherington HP, Shulman RG (1987) Combined  $^1\text{H}$  and  $^{31}\text{P}$  NMR studies of the rat brain in vivo: effects of altered intracellular pH on metabolism. *Ann NY Acad Sci* 508:81-88
- Brierley JB (1976) Cerebral hypoxia. In: *Greenfield's Neuropathology* (Blackwood W, ed), London, Edward Arnold, pp 46-47
- Bright GR, Fisher GW, Rogowska J, Taylor DL (1987) Fluorescence ratio imaging microscopy: temporal and spatial measurements of cytoplasmic pH. *J Cell Biol* 104:1019-1033
- Brown AW (1977) Structural abnormalities in neurones. *J Clin Pathol [Suppl] (R Coll Pathol)* 11:155-169
- Cammermeyer J (1961) The importance of avoiding "dark" neurons in experimental neuropathology. *Acta Neuropathol* 1:245-270
- Chang L-H, Pereira BM, Keniry MA, Murphy-Boesch J, Litt L, Weinstein PR, James TL (1987) Comparison of lactate concentration determinations in ischemic and hypoxic rat brains by in vivo and in vitro  $^1\text{H}$  NMR spectroscopy. *Magn Res Med* 4:575-581
- Clowes GHA, Hopkins AL, Simeone FA (1955) A comparison of the physiological effects of hypercapnia and hypoxia in the production of cardiac arrest. *Ann Surg* 142:446-460
- Cohen Y, Sanada T, Nishimura MC, Pitts LH, Chang L-H, Weinstein PR, James TL (1989) Surface coil spectroscopic imaging: time and spatial evolution of lactate following fluid percussion, a focal brain injury. Society of Magnetic Resonance in Medicine Eighth Annual Meeting, p 470
- Corbett RJ, Lupton AR, Hassan A, Nunnally RL (1988) Quantitation of acidosis in neonatal brain tissue using the  $^{31}\text{P}$  NMR resonance peak of phosphoethanolamine. *Magn Reson Med* 6(1):99-106
- Eisele JH, Eger EI, Maullem M (1967) Narcotic properties of carbon dioxide in the dog. *Anesthesiology* 28:856-865
- Folbergrová J, Siesjö BK (1973) Regulatory mechanisms affecting carbohydrates in the brain in hypercapnic acidosis. *Acta Physiol Scand* 88:281-283
- Frumin MJ, Epstein RM, Cohen G (1959) Apneic oxygenation in man. *Anesthesiology* 20:789-798
- Hillered L, Ernster L, Siesjö BK (1984) Influence of in vitro lactic acidosis and hypercapnia on respiratory activity of isolated rat brain mitochondria. *J Cereb Blood Flow Metab* 4:430-437
- Hopkins AL, Anzola J, Clowes GHA (1954) A quantitative experimental comparison of the effects of severe hypercapnia on the brain and heart. In: *Surgical Forum, Clinical Congress of the American College of Surgeons*, Philadelphia, WB Saunders, pp 736-739
- Litt L, González-Méndez R, Severinghaus JW, Hamilton WK, Shuleshko J, Murphy-Boesch J, James TL (1985) Cerebral intracellular changes during supercarbia: an in vivo  $^{31}\text{P}$  nuclear magnetic resonance study in rats. *J Cereb Blood Flow Metab* 5:537-544
- Mabe H, Blomqvist P, Siesjö BK (1983) Intracellular pH in the brain following transient ischemia. *J Cereb Blood Flow Metab* 3:109-114
- Matakas F, Birkle J, Cervos-Navarro J (1978) The effect of prolonged experimental hypercapnia on the brain. *Acta Neuropathol* 41:207-210
- Moon RB, Richards JH (1973) Determination of intracellular pH by  $^{31}\text{P}$  magnetic resonance. *J Biol Chem* 248:7276
- Nioka S, Chance B, Hilberman M, Subramanian HV, Leigh JS, Veech RL, Forster RE (1987) Relationship between intracellular pH and energy metabolism in dog brain as measured by  $^{31}\text{P}$ -NMR. *J Appl Physiol* 62:2094-2102
- Petroff OAC, Prichard JW, Behar KL, Alger JR, den Hollander JA, Shulman RG (1985) Cerebral intracellular pH by  $^{31}\text{P}$  nuclear magnetic resonance spectroscopy. *Neurology* 35:781-788
- Rehncrona S, Hauge HN, Siesjö BK (1989) Enhancement of iron-catalyzed free radical formation by acidosis in brain homogenates: difference in effect by lactic acid and  $\text{CO}_2$ . *J Cereb Blood Flow Metab* 9:65-70
- Safar P, Nemoto EM, Severinghaus JW (1973) Pathogenesis of central nervous system disorder during artificial hyperventilation in compensated hypercarbia in dogs. *Crit Care Med* 1:5-16
- Siesjö BK (1985) Acid-base homeostasis in the brain: physiology, chemistry, and neurochemical pathology. In: *Molecular Mechanisms of Ischemic Brain Damage—Progress in Brain Research* (Welsh FA, ed), New York, Elsevier, pp 121-154
- Siesjö BK, Bendek G, Koide T, Westerberg E, Wieloch T (1985) Influence of acidosis on lipid peroxidation in brain tissues in vitro. *J Cereb Blood Flow Metab* 5:253-258
- Taylor DJ, Bore PJ, Styles P, Gadian DG, Radda GK (1983) Bioenergetics of intact human muscle: a  $^{31}\text{P}$  nuclear magnetic resonance study. *Mol Biol Med* 1:77-94
- Westerhoff HV, van Dam K (1987) *Thermodynamics and Control of Biologic Free-Energy Transduction*. New York, Elsevier, pp 193-195